Uptake of Small Oxygenated Organic Molecules onto Ammonium Nitrate under Upper Tropospheric Conditions†

John E. Shilling, Brandon M. Connelly, and Margaret A. Tolbert*

CIRES and Department of Chemistry and Biochemistry, University of Colorado, Boulder, Colorado 80309-0216

Received: October 17, 2005; In Final Form: January 23, 2006

The uptake of formic (C_1), propanoic (C_3), butanoic (C_4), and pentanoic (C_5) acids onto ammonium nitrate (AN) has been investigated as a function of temperature and relative humidity using a Knudsen cell flow reactor coupled with FTIR−reflection absorption spectroscopy (FTIR−RAS). The uptake of acetone and methanol onto AN was also briefly studied. Initial uptake coefficients (γ) were determined over the temperature range 200−240 K. Formic, propanoic, and butanoic acids exhibited efficient but temperature-dependent uptake on AN, with larger uptake coefficients observed at lower temperatures. Pentanoic acid was not taken up by AN under any of the conditions studied. Uptake of acetone and methanol onto AN was observed, but in insignificant amounts under atmospherically relevant conditions. Infrared spectra revealed that propanoic and butanoic acids ionized on the surface, despite the fact that the AN films were effloresced. Formic acid reacted with the AN film to produce ammonium formate and ionized nitric acid. Adding small amounts of water vapor (4% RH) to the chamber resulted in dramatically increased γ values for all of the acids. Furthermore, the IR spectra showed the formation of a liquid layer when propanoic and butanoic acids adsorbed on the surface at RH = 20% and greater. Liquid water features were not observed at a similar relative humidity in the absence of the acids. These results show that small organic acids can be efficiently scavenged by AN and lead to enhanced water uptake under upper tropospheric conditions.

Introduction

Oxygenated organic molecules are now recognized to be ubiquitous constituents of the troposphere.[1] Measurements in the southern hemisphere have shown that oxygenated organic molecules are 5 times more abundant than nonmethane hydrocarbons, and photochemical models are unable to predict their atmospheric mixing ratios.[2] These oxygenated organic molecules influence the oxidative capacity of the atmosphere through interaction with photochemical HO_x and NO_x cycles, which, in turn, regulate tropospheric O_3 production.[3,4] In fact, one study found that HO_x production from the photolysis of acetone and peroxides, such as CH_3OOH, can be more important than HO_x production from the reaction of $O(^1D)$ with H_2O in the upper troposphere.[5] Therefore, it is important to understand the processes that control the gas-phase concentrations of these molecules.

On the basis of thermodynamic considerations, Barsanti and Panchow predict that small, monofunctionalized organic molecules with vapor pressures larger than $\sim 8 \times 10^{-5}$ Torr should not partition significantly into the aerosol phase through condensation or accretion reactions at 293 K.[6] Furthermore, Khan et al. measured the Henry's law coefficients of the C_1−C_6 monocarboxylic acids at 298 K and concluded that they were not soluble enough to partition significantly into the aqueous phase for liquid water contents typical of non-cloud aerosol.[7] The Henry's law coefficients of these acids are generally much larger than those of other small, monofunctional organic molecules such as methanol and acetone.[8] In light of these studies, other removal processes, such as rainout and photochemical oxidation, rather than heterogeneous processing on aerosol particles, should be the dominant sinks of monocarboxylic acids and short-chain alcohols and ketones. However, single-particle MS studies have found that tropospheric aerosol particles often contain oxygenated organics internally mixed with inorganic sulfate or nitrate salt.[9,10] In particular, the formate, acetate, and propionate ions are often prevalent in the negative-ion spectra.[11] These ions might be fragments of larger oxygenated organic ions or peroxides; however, they might also indicate the presence of formic, acetic, and propanoic acids in the aerosol phase.[11]

Carboxylic acids are one class of oxygenated organics that have received increasing attention in the literature in the past decade. They are a large fraction (25%) of the nonmethane hydrocarbon loading and are prevalent in a both urban and remote atmospheres.[12,13] Formic acid is the most prevalent organic acid in the gas phase, followed by acetic acid.[13] In urban environments, average mixing ratios of formic acid are 3−6 ppbv[14] and can be as high as 20 ppbv.[15] In remote rural regions, the median mixing ratio of formic acid is 5 ppbv and can exceed 10 ppbv.[16] In some regions, the mixing ratio of formic acid can exceed those of HNO_3 and HCl.[14] Formic and acetic acids are responsible for a significant portion of the free acidity in rainwater: up to 35% in North America[17] and up to 64% in more remote regions.[18] Formic acid is also believed to be an important sink for OH radicals in cloudwater, and, as such, it influences oxidation of other important atmospheric species such as SO_2.[19] Levels of propanoic and butanoic acids are lower but still significant, in the ranges 300−700 and 100−300 ppt, respectively.[20] Acetone and methanol are also present at significant concentrations in the atmosphere and are believed

* To whom correspondence should be addressed. E-mail: Tolbert@colorado.edu.

† Part of the special issue "David M. Golden Festschrift".

10.1021/jp055940q CCC: $33.50
Published on Web 03/15/2006

to participate in the NO_x and HO_x cycles.[2] Levels of acetone and methanol in the free troposphere are on the order of 500 and 700 pptv, respectively.[1]

Ammonium nitrate (AN) is an important regional air pollutant in areas where agricultural ammonia emissions mix with urban HNO_3 emissions. AN has been identified as a major constituent of the aerosol near urban centers such as southern California and Colorado's Front Range.[21−26] In these areas, AN is often the dominant aerosol component. For example, in Denver during the winter months AN has been found to comprise 25% of the total $PM_{2.5}$ and to be the single largest contributor to the total aerosol loading.[27] In contrast, ammonium sulfate was only 10% of the total $PM_{2.5}$ during the same time period.[27] At other locations along the Front Range, AN was responsible for even larger portions of the total $PM_{2.5}$ mass.[27] As a regional pollutant, AN is most important for its affect on visibility reduction in these areas. Studies have estimated that AN is responsible for 40% of the light scattering in Los Angeles[28] and 17% of the light scattering in Denver.[29] The scattering efficiency is related to the particle size, which, in turn, is controlled to a large extent by the water content of the aerosol. Therefore, it is important to understand the hygroscopic properties of aerosols.

Because of the low volatilities and high water solubilities of dicarboxylic acids, their effects on the hygroscopicity of inorganic salts have been extensively investigated.[30−34] In contrast, there are only a few studies on the effects of monocarboxylic acids on the hygroscopicity of inorganic salts.[35,36] In a previous report, we investigated the uptake of acetic acid onto AN films as a function of temperature and relative humidity and examined its effect on the water content of the AN film.[35] In this article, we extend the previous study to include all of the C_1-C_5 monocarboxylic acids. We also briefly examine the uptake of acetone and methanol onto the AN films. We compare the behavior of these molecules to our previous results and look for correlations between the uptake behavior and the physical properties of the organic compounds.

Experimental Section

Experiments were conducted in a high-vacuum stainless steel Knudsen cell equipped for FTIR−reflection absorption spectroscopy (FTIR−RAS). This apparatus has been described in detail previously.[37] Using this instrument, the gas phase is probed with mass spectrometry while the condensed phase is simultaneously monitored with FTIR−RAS. Water vapor partial pressures are monitored with a Baratron capacitance manometer. AN films are synthesized in situ by vapor deposition of HNO_3 onto a gold substrate followed by neutralization with NH_3. Film deposition and the general experimental procedure have been detailed previously.[35] The spectra of the resultant films match literature spectra of crystalline AN.[38] There is no evidence of liquid water in the spectra of the AN films.

Initial uptake coefficients (γ) and coverages (θ) were calculated from the MS data. Uptake coefficients are calculated according to eq 1

$$\gamma = \frac{A_h(S_0 - S)}{A_s S} \quad (1)$$

where S is the MS signal at the point of interest, S_0 is the original MS signal, A_h is the calibrated area of the escape orifice (0.19 cm^2), and A_s is the surface area of the substrate (5.07 cm^2). The number of molecules taken up by the film is determined by integrating the area under the uptake curve and multiplying this area by a calibration factor. The calibration factor is determined from the relationship of the MS signal to the Baratron. Briefly, variable amounts of the pure gas are leaked into the chamber while the gas pressure and the MS signal of a representative ion (e.g., m/z 74 for propanoic acid) are simultaneously recorded. A plot of the MS signal against the Baratron pressure is linear over several orders of magnitude. A linear regression forced through the data yields the calibration factor. Coverages are then obtained by dividing the uptake by the surface area of the substrate. Coverages are converted monolayer units (ML) by dividing the absolute coverage by the monolayer density. The monolayer density was calculated from the liquid density as previously described.[35] In all calculations, the geometric surface area of the gold substrate (5.07 cm^2) was used to approximate the surface area of the sample.

TABLE 1: Physical Constants of Trace Gases Studied in This Work

gas	MW (g/mol)	BP[a] (°C)	water solubility[b] (g/mL)	pK_a[c]	H[d] (mol/atm·L)
methanol	32	64.5	miscible		219.8
acetone	58	56.2	miscible		53.5
formic acid	46	100.5	miscible	3.75	5530
acetic acid	60	118	miscible	4.76	
propanoic acid	74	141	miscible	4.86	5502
butanoic acid	88	164	miscible	4.83	4227
pentanoic acid	102	187	4.97	4.84	2232

[a] Reference 43. [b] Data for pentanoic acid from reference 62. All other data from reference 8. [c] Reference 8. Data for formic acid at 293 K. Data for other acids at 298 K. [d] Data for acids at 298 K from reference 7. Other data at 298 K from reference 43.

Bulk experiments to estimate the room-temperature deliquescence relative humidity (DRH) values of select ammonium/organic acid salt combinations were also conducted. In these experiments, ammonia/organic acid salt mixtures were dried under a vacuum and then exposed to varying RHs in a glass vacuum line until deliquescence was visually observed. The RH was set by varying the temperature of a known composition of sulfuric acid/H_2O solution that had been degassed by several freeze−pump−thaw cycles. The RH above the sulfuric acid solution was measured with the Baratron and verified using the AIM model and the known acid composition.[39−41] Ammonium formate and ammonium acetate were obtained commercially and used without further purification. Ammonium propionate was synthesized by bubbling anhydrous ammonia gas through a solution of ACS grade propanoic acid. The product was then purified by recrystallization in ethanol and dried on the vacuum line before use. Ammonium butyrate was also synthesized, but it rapidly decomposed back to ammonia and butanoic acid under laboratory conditions; therefore, it was not tested. This method of determining the bulk DRH was adopted over methods previously used in our laboratory to avoid interferences caused by the high vapor pressures of ammonia and organic acid above the salt crystals.[31,42]

Results and Discussion

Relevant physical constants of each trace gas studied are listed in Table 1.[7,8,43] As can be seen, we have investigated the role of functional group and carbon chain length on the uptake properties. The significance of the physical properties of the molecules in predicting their uptake behavior is discussed in detail in subsequent sections.

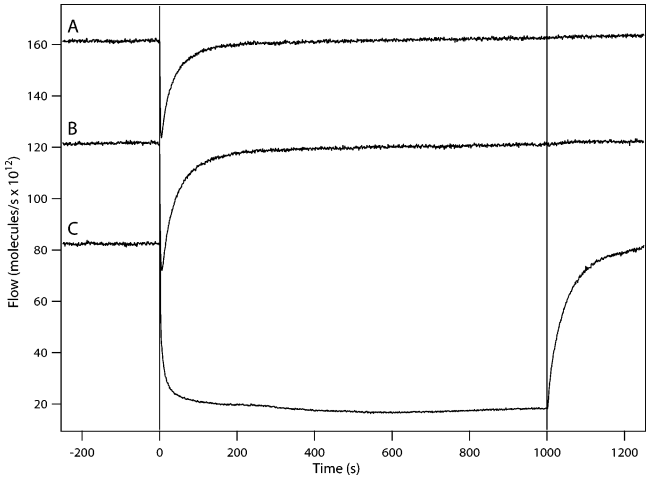

Figure 1. Mass spectral data obtained for propanoic acid adsorption onto AN. Traces A and B show the uptake of propanoic acid onto AN in the absence of additional water vapor at 220 and 210 K, respectively. Trace C shows the uptake onto an AN film at 210 K and 39% RH. Vertical lines have been drawn at $t = 0$ s and at $t = 1000$ s to shown when the substrate was exposed to and isolated from the gas-phase acid. Traces have been offset for clarity.

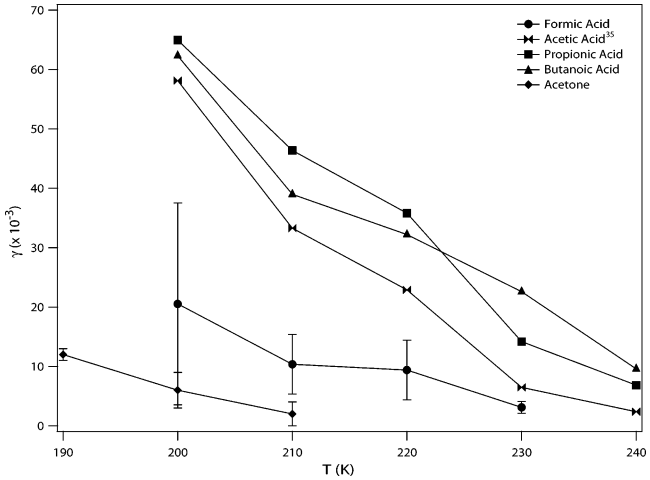

Figure 2. Initial uptake coefficients (γ) obtained for the uptake of trace gases onto crystalline AN films. Error bars at the 95% confidence limit have been added to the formic acid and acetone data. Error bars for the other acids, which are omitted for clarity, are well represented by the magnitude of the formic acid error bars.

Figure 1 illustrates calibrated MS traces for the uptake of propanoic acid onto AN under various conditions. These data are representative of the uptake behavior observed in this study. Vertical lines in Figure 1 indicate the points in the experiment when the AN film was exposed to and isolated from the trace gas. As was the case with acetic acid, we observe three distinct uptake behaviors in this study: saturated uptake (trace A), unsaturated uptake with partial recovery (trace B), and unsaturated uptake with no recovery (trace C).[35] Saturated uptake (trace A) is marked by recovery of the MS signal to its original level prior to isolation of the film from the gas phase. Saturated uptake was observed for methanol and acetone under all conditions studied and for the carboxylic acids at $T > 210$ K. Unsaturated uptake with partial recovery (trace B) is marked by a recovery of the MS signal to a level slightly below its original level prior to isolation of the film from the gas phase. The MS signal subsequently recovers to its original level when the film is isolated from the gas phase. Unsaturated uptake with partial recovery was observed for the carboxylic acids at 200 K. Uptake did not fully saturate at 210 K in half of the experiments for each species of carboxylic acid. However, the initial uptake coefficients for a particular species at 210 K were similar, regardless of whether uptake saturated. Unsaturated uptake with no recovery (trace C) is marked by no recovery of the MS signal prior to isolation of the film from the gas phase. Unsaturated uptake with no recovery was observed in the carboxylic acid experiments when water vapor was added to the chamber. A more detailed discussion of these behaviors was published previously.[35] Blank experiments were conducted in which no AN film was deposited onto the gold substrate. In these experiments, no change in the MS signal was observed upon opening or closing the cup. This indicates that no uptake occurred on the gold under conditions identical to those used in experiments.

Figure 2 shows the initial uptake coefficients obtained for the uptakes of acetone, formic acid, propanoic acid, and butanoic acid on crystalline AN as a function of temperature. Error bars at the 95% confidence limit have been added to the formic acid and acetone data. Error bars for the other acids, which have been omitted for clarity, are similar in magnitude to the formic acid error bars. Also shown for comparison are data for the uptake of acetic acid onto AN under similar conditions.[35] For all experiments shown, no additional water vapor was introduced into the vacuum chamber. As seen in Figure 2, the uptake of the C_1-C_4 monocarboxylic acids onto AN is much more efficient across the entire temperature range than the uptake of acetone. All of the uptake coefficients increase with decreasing temperature. The initial uptake coefficients for the C_2-C_4 acids are the same within error and vary from $\gamma = 0.062$ at 200 K to $\gamma = 0.002$ at 240 K. However, the γ values of the C_2-C_4 acids are roughly 3 times greater than the γ values of formic acid, which range from $\gamma = 0.02$ at 200 K to $\gamma < 0.001$ at 240 K. At 200 K, the γ values of C_2-C_4 acids approach the literature value of $\gamma = 0.067$ for the uptake of acetic acid onto water at 273 K and exceed the literature value of $\gamma = 0.047$ for formic acid uptake onto water at the same temperature.[44] In the Atmospheric Implications section of this work, we show that these γ values are sufficiently large that uptake of the acids onto crystalline AN can compete with other removal processes. Previous results showed that the γ values for acetic acid uptake onto AN are independent of the acetic acid partial pressure.[35] We have confirmed that this is also true of butanoic acid uptake onto AN. Therefore, we assume that γ is independent of pressure for all molecules discussed in this work, although they have not all been explicitly tested.

The uptake of methanol was below the detection limit of $\gamma = 1 \times 10^{-3}$ for temperatures above 180 K. The uptake of pentanoic (C_5) acid was below the detection limit over the temperature range 200−240 K. These low values of γ indicate that the heterogeneous loss of methanol and pentanoic acid onto AN is slow and unlikely to compete with other removal processes.

Coverages of the acids on the AN films were also determined. The coverages of the acids ranged from $\theta = 50$ ML at 200 K to $\theta = 2$ ML at 240 K. However, saturated uptake was never observed at 200 K and was observed in only half of the experiments at 210 K. Therefore, the stated coverage at 200 K represent the amount of acid taken up after 1000 s of exposure and is limited by the dose and uptake coefficient. Nevertheless, the coverages of all the acids are at least several monolayers, indicating a significant amount of organic can partition onto dry AN. Uptake of acetone saturated under these conditions. The saturated coverages for acetone were much smaller than

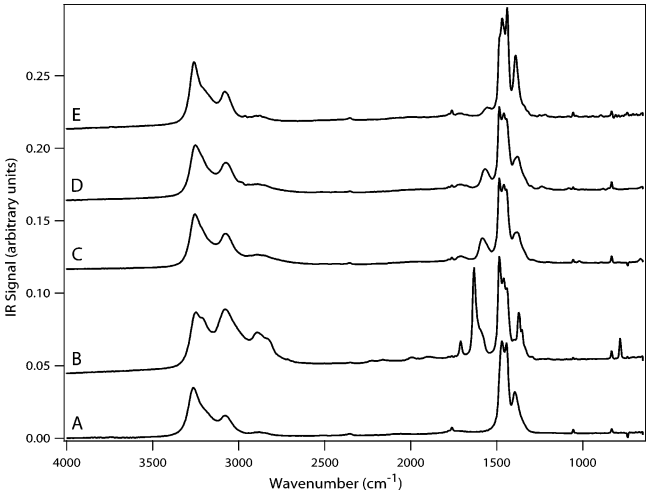

Figure 3. IR spectra of reaction products of AN and the gases studied in this work. Spectrum A shows crystalline AN at the beginning of the experiments. Spectra B−E show AN after exposure to formic, acetic,[35] propanoic, and butanoic acids, respectively, at 200 K. Spectra have been offset for clarity.

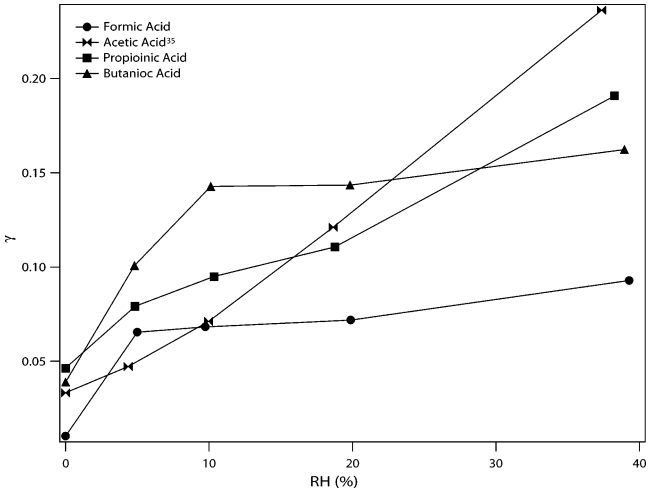

Figure 4. Initial uptake coefficients obtained for the uptake of trace gases onto AN at 210 K as a function of RH.

those for the acids, ranging from $\theta = 0.14$ to $\theta = 0.02$ ML from 190 to 210 K. At temperatures above 210 K, the coverage dropped below the detection limit of $\theta = 0.01$ ML. These small equilibrium coverages indicate that AN is unlikely to be a significant sink of acetone in the atmosphere. The lower coverage of acetone relative to the acids is likely due to the fact that the uptake of acetone is physical in nature whereas the uptakes of the acids are reactive, as discussed in subsequent sections.

The IR spectra of the reaction products of the various organic acids and the AN films are shown in Figure 3. The lowermost spectrum is of AN and is shown for reference. As can be seen in Figure 3, the spectrum of the formic acid reaction products is markedly different from the spectra of the C_2-C_4 reaction products. Throughout this investigation, the reaction of formic acid with the AN film was distinctly different from that of the other acids. IR spectra relevant to formic acid uptake onto the AN films will be examined in more detail later in this manuscript. The most noticeable change in the spectra of the C_2-C_4 acid reaction products is the strong peak from 1580 to 1550 cm^{-1}. We have attributed this peak to the stretching mode of the carboxylate ions.[45] We note that this peak red shifts by $\sim$10 cm^{-1} for each additional CH_2 unit added to the molecule. Spectral features indicative of un-ionized acid molecules are absent from the spectra.[45] A weak feature is also present at 1708 cm^{-1} in these spectra. We have attributed this peak to the bending mode of the H_3O^+ ion based on its intensity and on literature spectra.[46] The C═O stretching mode of the un-ionized acids also absorbs here, so it is possible that a small number of molecules remain physisorbed to the surface in the molecular state.[45] However, this peak does not shift with increasing carbon chain length as would be expected if it were the C═O stretching mode signature. Therefore, we believe that the 1708 cm^{-1} peak is actually the H_3O^+ ion stretch and that no molecular acid is present.

To extend the atmospheric relevance of this study, experiments were conducted at a constant temperature of 210 K as a function of relative humidity. During these experiments, the AN film was isolated from the chamber, and water vapor was added to the chamber and allowed to reach equilibrium with the walls as determined with the Baratron. Relative humidity was calculated by referencing this water vapor partial pressure to the saturation vapor pressure of water, as determined using the Wexler expression.[47] In select experiments, the AN was exposed to the water vapor for several minutes before being isolated from the chamber atmosphere. These experiments yielded results identical to those obtained in experiments in which the AN film was not preexposed to water vapor. The organic acid of choice was then added and monitored with the MS, and experiments were conducted as before.

Figure 4 shows the γ values obtained for each acid as a function of increasing relative humidity at 210 K. As seen in Figure 4, all of the γ values increase rapidly as a function of relative humidity, and some reach a plateau at RH > 20%. This plateau corresponds to the upper limit of detection for γ of the instrument. All of the γ values determined in this study approach or exceed $\gamma = 0.1$ at RH > 20%. In the free troposphere, RH rarely drops below 20%. These large γ values indicate that the uptake of the acids onto the film at atmospherically relevant relative humidities is efficient, with $\sim$10% of the collisions resulting in reaction. In fact, these values exceed the γ determined for the uptakes of acetic and formic acids onto pure liquid water droplets at 273 K.[44] In the Atmospheric Implications section, we present calculations suggesting that uptake of the C_1-C_4 acids onto AN might be a dominant removal pathway for the acids.

The most dramatic effect of the addition of water vapor during these experiments was to shift the uptake regime from saturated to unsaturated with no recovery regime. This shift occurred at RH = 4%. At this point, essentially all of the acid flowing into the chamber is taken up onto the AN film. Again, coverage under unsaturated conditions is limited only by the dose and uptake coefficient. For similar doses, the coverages of the monocarboxylic acids increased by factors of 5−25 when RH was increased from RH < 0.1% to RH = 40%. A small number of experiments were run over longer time scales (4000 s) without any indications of saturation. The coverage data again indicate that significant amounts of these carboxylic acids can partition into the aerosol phase under atmospherically relevant RHs.

As before, examination of the IR spectra of the condensed phase provides insight into the reaction process. The spectra of the acid reaction products and an AN reference spectrum, all at RH = 40%, are shown in Figure 5. The AN spectrum at RH = 40% is identical to that at RH < 0.1%, indicating a lack of water uptake by the pure AN film at this RH. As was the case with adsorption onto the crystalline films, peaks were observed to grow in the IR spectra of the C_2-C_4 reaction products from

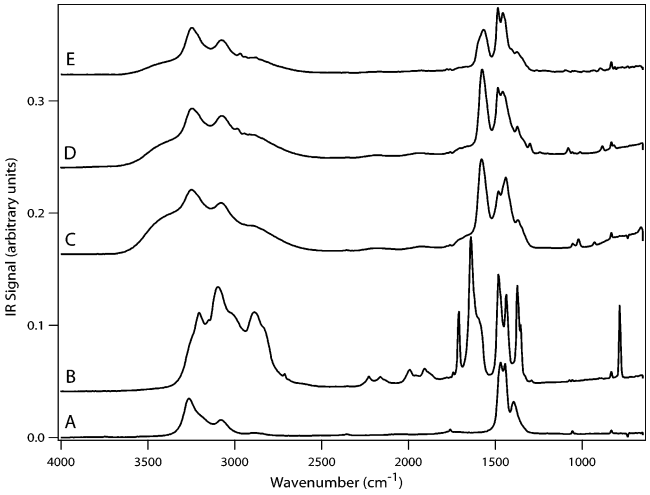

Figure 5. IR spectra of the reaction products of AN and the gases studied in this work. All spectra were recorded after 1000 s of exposure of the gas at 210 K and ~40% RH. Spectrum A shows the AN film. Spectra B−E show the AN film after uptake of formic, acetic,[35] propanoic, and butanoic acids, respectively. Spectra have been offset for clarity.

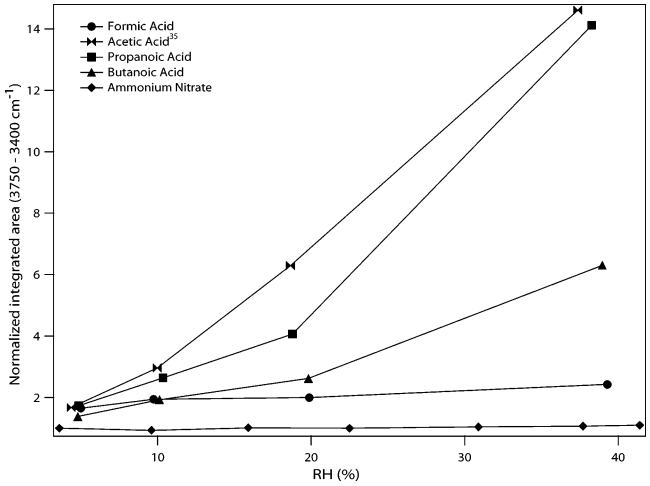

Figure 6. Integrated area of the liquid water stretching region from 3750 to 3400 cm^{-1} as a function of RH and trace gas. Areas have been normalized to the 0% RH point of ammonium nitrate and were determined after 1000 s of trace gas exposure at 210 K.

1580 to 1550 cm^{-1}. Again, these peaks are characteristic of carboxylate ion stretches.[45] The H_3O^+ ion bending mode is also observed in these spectra at 1708 cm^{-1}.[46] However, the most dramatic changes in the IR spectra at 40% RH are the broad peaks centered around 3400 and 700 cm^{-1}. These peaks are characteristic of the OH stretch and libration, respectively, of liquid water. These features are completely absent from the reference spectrum of AN at the same relative humidity in the absence of the organic acids. From these spectra, it is clear that the adsorption of the organic acids increases the liquid water content of the AN film.

To better quantify the effects of the organic acids on the water content of the films, the integrated area of the OH stretching region of liquid water (3750−3450 cm^{-1}) is plotted as a function of relative humidity for each acid in Figure 6. These integrated areas have been normalized to the AN 0% RH point. As seen in Figure 6, there is no change in the liquid water region of the spectrum when the AN film is subjected to increasing relative humidity in the absence of the acids. This observation is consistent with a trajectory on the lower side (deliquescence

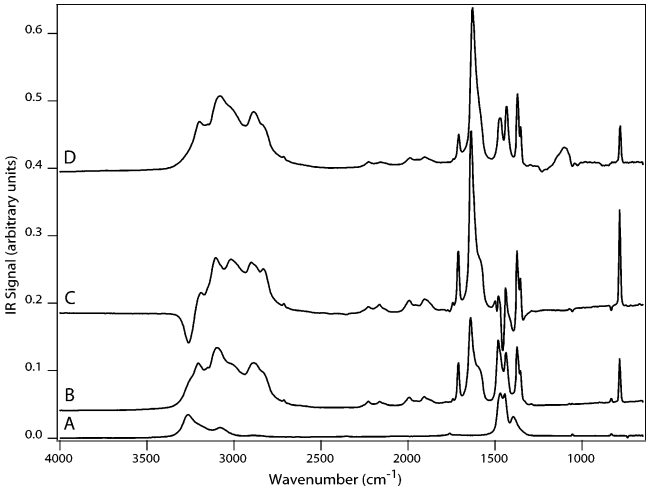

Figure 7. IR spectra detailing the reaction of formic acid with AN at 210 K and 40% RH. Spectrum A shows the AN film at the start of the experiment. Spectrum B shows the reaction products of formic acid and AN after 1000 s of exposure at 210 K and 40% RH. Spectrum C shows the subtraction of spectrum A from spectrum B. Spectrum D shows a reference spectrum of ammonium formate prepared in the chamber from gas-phase precursors.

branch) of the AN hygroscopic growth curve. The deliquescence of RH of AN has been reported to be 62% at room temperature,[48] and a thermodynamic model predicts that the DRH increases rapidly as temperature decreases.[49] In light of these two facts, it is not surprising that liquid water features are absent from this spectrum at 40% RH. However, the water content of the AN film increased dramatically as the organic acids were taken up by the film. The effect was most dramatic for the uptake of acetic and propanoic acids. Assuming that the area of this peak is linear with respect to the liquid water content of the film, the uptake of propanoic and acetic acids enhanced the AN film's liquid water content by a factor of 14 at 40% RH. Assuming that the oscillator strength for the water OH stretch is constant in the various acid/AN/water solutions, the uptake of butanoic acid enhanced the water content of the film by roughly half as much as the uptake of acetic and propanoic acids. The uptake of formic acid onto the AN film did not increase the film's liquid water content.

As seen in Figure 5, the IR spectra of the reaction products of formic acid appear markedly different from the spectra of the C_2−C_4 reaction products. Several IR spectra detailing the reaction of formic acid with the AN film are shown in Figure 7. Spectrum A shows the AN film before exposure to the formic acid. Spectrum B shows the reaction products on the same film after 1000 s of reaction time at 40% RH. By comparison with the other reaction product spectra (Figure 5), one can see that there are more peaks present in this spectrum and that the peaks are much sharper in appearance. Furthermore, the peaks associated with liquid water are absent. Spectrum C shows the subtraction of spectrum A from spectrum B. In this subtraction spectrum, one can see that there are now negative peaks in the NH stretching region at 3263 cm^{-1}, in the NH bending region at 1454 and 1488 cm^{-1}, and in the nitrate stretching region at 1392 cm^{-1}. These negative peaks show that the AN film is being consumed in the reaction. Spectrum D shows a film of ammonium formate prepared by condensing formic acid on the gold substrate and neutralizing it with gas-phase ammonia. A comparison of spectra D and B shows that crystalline ammonium formate is produced when formic acid is taken up by the AN film. There is no evidence for the formation of molecular

nitric acid in the spectrum. Instead, we see changes in the nitrate stretching region. Unfortunately, ammonium formate also absorbs in this region of the IR, making further conclusions about the nature of the substrate/nitrate interaction difficult. We tracked the nitric acid signal during the reaction with the MS and observed that nitric acid is not released into the gas phase as the reaction proceeds. However, if the flow of formic acid is turned off and the film is heated, HNO_3 desorbs into the gas phase at a temperature of approximately 240 K. No release of nitric acid to the gas phase is observed under these conditions for pure AN films. Indeed, the vapor pressure of nitric acid above an AN film is negligibly small, 2×10^{-9} Torr, at 240 K.[50] In light of these observations, we hypothesize that nitrate is initially present in some weakly bound state that is destabilized upon heating, releasing nitric acid into the gas phase.

The IR observation of nearly complete ionization of these acids on the AN film is somewhat surprising. The pK_a's of the carboxylic acids studied in this work at room temperature are listed in Table 1. We are unaware of any measurements of the pK_a's of these acids over the temperature range studied in this work. However, temperature-dependent dissociation constants (K_a's) are available in the literature over the temperature range 273−333 K for formic, acetic, propanoic, and butanoic acids.[51−54] These data show that K_a decreases slightly with decreasing temperature below ~296 K. If extrapolation of this trend below the measured range is valid, the small values of K_a suggest that much of the acid should remain in its molecular form, even at low temperature. Furthermore, the uptake of formic acid, which dissociates to a greater extent than the other acids, was significantly less efficient than the uptake of the other acids. Therefore, to reconcile the IR observations with the available thermodynamic data, reactions in addition to ionization must occur on the surface of the AN film.

In light of the spectral evidence and the dependence of all the carboxylic acid γ values on RH, we hypothesize that eq 2 represents the overall chemical reaction taking place when the monocarboxylic acids are taken up by the AN film.

$$\mathrm{RCOOH(g) + H_2O(l) + NH_4NO_3(s) \rightarrow NH_4RCOO(s) + H_3O^+(aq) + NO_3^-(aq)} \quad (2)$$

Formation of the ammonium/carboxylic acid salt in the crystalline state was observed only in the case of ammonium formate. When the C_2-C_4 monocarboxylic acids were taken up by the AN film, we observed the formation of their respective carboxylate ions. Therefore, we believe that for these acids the crystalline salt is a short-lived intermediate and reaction 2 is immediately followed by reaction 3

$$\mathrm{NH_4RCOO(s) \xrightarrow{H_2O} NH_4^+(aq) + RCOO^-(aq)} \quad (3)$$

We note that no liquid water features are observed in the IR spectra of the reaction products in the absence of additional water vapor (Figure 3); therefore, we believe that the ammonium/organic salts are present in a thin, metastable aqueous layer overlaying crystalline AN under low-RH conditions. In this case, the (l) phase indicator after the water in eq 2 is meant to signify surface-adsorbed water. No bulk liquid water is associated with the ammonium/organic salt system under these low-RH conditions. In the case of formic acid, the adsorbed nitrate and hydronium ions can then recombine to form nitric acid and water, which is released into the gas phase upon heating, as shown in eq 4.

$$\mathrm{H_3O^+(aq) + NO_3^-(aq) \rightarrow HNO_3(l) + H_2O(l) \rightarrow HNO_3(g) + H_2O(g)} \quad (4)$$

To confirm the plausibility of eq 2, we calculated its heat of reaction from the heats of formation of the products and reactants. The heats of formation of many of the reaction products are available in the literature.[8,55] The heats of formation of H_3O^+ and NO_3^- were determined from the heat of ionization of nitric acid[56] and the heats of formation of water and nitric acid.[8] All relevant thermodynamic quantities are listed in Table 2. Using the heats of formation listed in Table 2, we calculate that $\Delta H_r = -12.3$ kJ/mol for the reaction of formic acid with AN. Similarly, $\Delta H_r = -6.4$ kJ/mol for the reaction of acetic acid with AN. These calculations show that the reactions of acetic and formic acids with AN, as shown in eq 2, are thermodynamically favorable. Furthermore, the formic acid reaction is slightly more exothermic than the reaction of acetic acid with AN. Unfortunately, the heats of formation for the ammonium salts of propanoic and butanoic acids are unavailable, so we are unable to calculate the thermodynamics for the reaction of these gases with AN.

TABLE 2: Heats of Formation Used in the Thermodynamic Calculations Presented in the Text

species	ΔH_f (kJ/mol)
$H_2O(l)$	−258.8[a]
$HNO_3(l)$	−174.1[a]
HCOOH(g)	−378.7[a]
$CH_3COOH(g)$	−432.2[a]
$NH_4NO_3(s)$	−365.5[a]
$NH_4HCOO(s)$	−568.2[b]
$NH_4CH_3COO(s)$	−616.6[b]
$NO_3^-(aq) + H_3O^+(aq)$	−446.3[c]

[a] Reference 8. [b] Reference 55. [c] Calculated from ΔH_f values of water and nitric acid and the heat of ionization of nitric acid. $\Delta H_i = -13.4$ kJ/mol at 273 K for nitric acid.[56]

In the absence of water, the reactions of formic and acetic acids with AN, as shown in eq 5, are endothermic

$$\mathrm{NH_4NO_3(s) + RCOOH(g) \rightarrow NH_4RCOO(s) + HNO_3(l)} \quad (5)$$

and the amount of surface-adsorbed water limits the uptake. There are reports in the literature supporting the existence of such layers of surface-adsorbed water on inorganic salts below their DRH.[57−60] Once all of the available water is consumed, the uptake is no longer thermodynamically favorable and halts. Thus, saturated uptake is observed on the crystalline AN films in experiments in which water vapor is not added to the chamber.

When additional water vapor is added to the chamber, liquid water features grow into the IR spectra as the C_2-C_4 acids are taken up by the AN film. Although the DRH of pure AN is above the experimental RH, it is clear from the spectra that the DRHs of the AN/C_2-C_4 acid reaction products are lower than the experimental RH. No liquid water features were observed in the IR spectra when formic acid was taken up by the AN film. Therefore, we believe that the ammonium salts formed from reaction of the C_2-C_4 acids with AN are deliquescent under the experimental conditions whereas the ammonium salt of formic acid is not.

To test this hypothesis, we measured the bulk deliquescence relative humidities of several ammonium salts relevant to this work at 298 K. The results of these measurements are reported

TABLE 3: Water Solubility, ΔH_{sol}, and DRH at 298 K for Ammonium Salts Studied in This Work

salt	water solubility[a] (g/100 g of H_2O)	ΔH_{sol}[a,b] (kJ/mol)	DRH at 298 K (% water)
NH_4NO_3	213	25.69	62[c]
NH_4CHOO	143	27.2	47
NH_4CH_3COO	148	−2.38	36
$NH_4C_2H_5COO$			40

[a] Reference 8. [b] Data for ammonium formate calculated from solubility data available on NIH toxnet database.[43] [c] Literature value of the DRH of AN is 62%.[48]

in Table 3, along with the water solubility and ΔH_{sol} for each salt. Because literature values are available for the DRH of AN, these data can be used to validate the accuracy of our method for determining the DRHs of the salts. As can be seen in Table 2, we obtained a DRH of 62% for the pure AN solution. This value is in excellent agreement with the literature value of 62% at room temperature.[48] The room-temperature DRH values for all ammonium/organic acid salt systems determined in this work are lower than that of AN. In addition, the DRHs of ammonium acetate and ammonium propionate are lower than the highest RH studied in the uptake experiments (~40%), whereas the DRH of ammonium formate is above this value. Therefore, to first order, the hypothesis that the uptakes of acetic, propanoic, and butanoic acids on AN produce deliquescent salts is confirmed. Similarly, these results confirm that the ammonium formate produced from the reaction of formic acid and AN should remain crystalline under the conditions studied herein. It is of note that the water solubility of the salts alone is a poor predictor of hygroscopicity.

The above DRH data were collected at 298 K. The thermodynamic model of Tang and Munkelwitz predicts that the change of a salt's DRH with temperature is a function of its water solubility and latent heat of solution, as shown in eq 6

$$\ln \mathrm{DRH}(T) = \ln \mathrm{DRH}(T_m) + \frac{1}{R}\int_{T_m}^{T} \frac{n(T)\,\Delta H_{sol}(T)}{T^2}\,\mathrm{d}T \quad (6)$$

where $\mathrm{DRH}(T_m)$ is the measured room-temperature DRH, R is the gas constant, $n(T)$ is the water solubility of the salt, and $\Delta H_{sol}(T)$ is the salt's heat of solution.[61] The DRHs of the salts at 210 K can thus be estimated from the parameters listed in Table 3. Using the room-temperature value of the solubility, we calculate that the DRH of ammonium acetate is 31% at 210 K. The DRH of ammonium formate is greater than 100% RH at 210 K. Note that the solubility is also temperature-dependent and should scale with the heat of solution. Thus, the DRH of ammonium acetate should be even lower than 31% at 210 K. This is in agreement with our observations of liquid water features in the spectra recorded during the uptake of acetic acid onto AN at RH = 20% and greater. Literature values for the heats of solution for the other carboxylic acid/ammonium salts are unavailable, so we are unable to conduct similar calculations for these salts.

It is somewhat surprising that pentanoic acid (C_5) was not taken up by the AN film under any of the conditions studied in this work. The Henry's law coefficient for pentanoic acid, shown in Table 1, is more than an order of magnitude higher than that of acetone, for which a small amount of uptake was observed. Furthermore, large quantities of butanoic acid, which has only one fewer CH_2 unit, were taken up by the film. The pK_a's for the C_2-C_5 acids are approximately equal (Table 1), so pentanoic acid should ionize to the same degree as the shorter-chain acids. The C_1-C_4 monocarboxylic acids are all reported to be miscible in water.[8,62] However, the water solubility of pentanoic acid is reported to be 4.97 g/100 g of H_2O.[62] The low water solubility and long hydrycarbon chain of pentanoic acid might prevent it from initially adsorbing to the surface. Alternatively, the thermodynamics of the overall reaction might be unfavorable once the hydrocarbon chain reaches a threshold length. The ΔH_r values for the uptakes of formic acid and acetic acid onto AN are given in the preceding paragraphs. In the case of these two carboxylic acids, the heat of reaction becomes less exothermic as the carbon chain length increases. Unfortunately, no literature data are available for the heats of formation for other monocarboxylic acid/ammonium salts. It is likely that the stability of these salts decreases with increasing hydrocarbon chain length. Indeed, we observed that ammonium butyrate decomposed back into ammonia and butanoic acid under laboratory conditions. Furthermore, the stability of the acids increases with increasing chain length.[8] Therefore, we believe that it is reasonable to conclude that the thermodynamics of the reaction of pentanoic acid with AN are unfavorable, preventing its uptake onto the film.

A molecule's water solubility and Henry's law coefficient have been used to identify organics that are likely to partition into the aerosol phase.[62] Although this seems useful for some organics compounds, such as the short-chain dicarboxylic acids, it is clear from our data that there are notable exceptions. Therefore, we conclude that water solubilities or Henry's law coefficients alone are poor predictors of monocarboxylic acids' ability to partition into the AN films. Instead, it seems that the detailed chemistry must be taken into account, most importantly, the properties of possible reaction products.

Finally, we analyzed the data with a precursor-mediated adsorption model as described in previous publications to determine ΔH_{obs} and ΔS_{obs} values.[35,44] Briefly, the quantity $\ln[\gamma/(1-\gamma)]$ is plotted against the reciprocal of the temperature. As shown in eq 7, ΔH_{obs} and ΔS_{obs} are extracted from the slope and intercept, respectively, of a line fit through the data plotted accordingly.

$$\ln\left(\frac{\gamma}{1-\gamma}\right) = -\frac{\Delta H_{obs}}{RT} + \frac{\Delta S_{obs}}{R} \quad (7)$$

We note that the values for ΔH_{obs} and ΔS_{obs} represent the difference in enthalpy and entropy between the transition state for species moving into the chemisorbed state from the physisorbed state and the transition state for physisorbed species moving to the gas phase.[63] Figure 8 shows the γ data plotted according to eq 7 and the linear regression fits for each trace gas. The values of ΔH_{obs} and ΔS_{obs} extracted from these fits are reported in Table 4. As seen in the table, many of the values are approximately equal with the exception of the ΔH_{obs} values for acetic acid and butanoic acid. As seen in Table 3, ΔH_{obs} for acetic acid is ~50% higher and ΔH_{obs} for butanoic acid is somewhat lower than the ΔH_{obs} values of the other gases. It is likely that these values reflect on the interaction of the hydrocarbon chain with the ionic lattice. As the hydrocarbon chain becomes longer, movement of the carboxylate ions into the AN film is increasingly disruptive of the AN lattice structure. The values of ΔS_{obs} follow a similar trend in magnitude, indicating increasing disorder of the chemisorbed carboxylate ions with increasing hydrocarbon chain length. Again, this could indicate an increasing disorder of the resultant lattice structure.

Atmospheric Implications

The main removal mechanism for organic acids is thought to be rainout, as removal rates with respect to photolysis[13] and

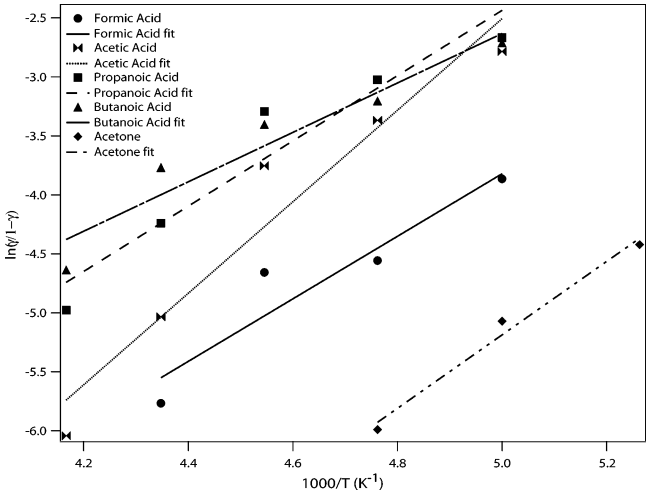

Figure 8. Fits of the temperature-dependent uptake coefficients for the trace gases studied in this work. Values of ΔH_{obs} and ΔS_{obs} were extracted from the slope and intercept of the fits, respectively, according to eq 7.

TABLE 4: Calculated Values of ΔH_{obs} and ΔS_{obs} for Trace Gas Uptake onto Crystalline AN Films

species	ΔH_{obs} (kJ/mol)	ΔS_{obs} (J/K·mol)
formic acid	−22.0	−142
acetic acid[a]	−32.3	−182
propanoic acid	−23.0	−135
butanoic acid	−17.4	−109
acetone	−25.9	−173

[a] Data for acetic acid from reference 35.

reaction with OH[64,65] are low. If we assume an AN aerosol surface area of between 16 and 550 $\mu m^2/cm^3$, we can calculate the lifetimes of the various acids with respect to heterogeneous removal from our γ values. Values of the AN surface area are derived from tropospheric measurements of AN aerosol[21] as described in previous work.[35] Using the γ values of formic acid determined in this work, which were lower than those of the other acids, we can estimate a lower limit for the lifetime with respect to heterogeneous removal. On the dry AN film, we obtained $\gamma = 0.01$ at 210 K. Under these conditions, the lifetime of formic acid in the kinetic limit is between 56 min and 35 h for the high and low limits, respectively, of the AN surface area. A similar calculation for formic acid at 210 K and 20% RH yields a heterogeneous lifetime of between 8 min and 5 h. These lifetimes are short compared to the lifetime of several days to weeks for removal by reaction with OH.[64,65] Therefore, we conclude that heterogeneous removal of these monocarboxylic acids can compete with these other removal mechanisms, even on crystalline AN.

We have shown that small, oxygenated organics can partition into the aerosol phase even under conditions of low RH. No correlation existed between the partitioning and a single thermodynamic property of the molecules. In the case of the monocarboxylic acids, it seems likely that the properties of the reaction products drive the partitioning and that the detailed chemistry of the system needs to be considered. However, this behavior was observed only for the monocarboxylic acids, which constitute only a fraction of the total non-methane hydrocarbon (NMHC) atmospheric mixture. For nonreactive species such as acetone and methanol, water solubility and the Henry's law coefficient do correlate with uptake behavior.

The uptakes of propanoic and butanoic acids dramatically enhanced the water content of the film. Liquid water features were observed to grow into the spectra at RH = 20% and greater when these acids were taken up by the film. These features were not observed in the absence of the acids. Therefore, AN aerosol that has been exposed to these acids might contain liquid water at lower RH than would the pure aerosol.

The reaction of formic acid with the AN film produced weakly bound HNO_3 and ammonium formate, which did not deliquesce. The nitric acid that was produced in this reaction desorbed from the film at 240 K. The vapor pressure of nitric acid above solid AN at 240 K is negligibly small.[50] Therefore, the reaction of formic acid with AN might represent a pathway for the revolitalization of HNO_3 at relatively low temperatures and might lead to the redistribution of NO_y.

Acknowledgment. This work was partially supported by the Biological and Environmental Research Program, U.S. Department of Energy, under Grant DE-FG03-01ER63096 and the National Science Foundation under Grant ATM-0137261. J.E.S acknowledges support from the NASA ESS fellowship (NGT5-30422).

References and Notes

(1) Singh, H. B.; Kanakidou, M.; Crutzen, P. J.; Jacob, D. J. *Nature* **1995**, *378*, 50.
(2) Singh, H.; Chen, Y.; Staudt, A.; Jacob, D.; Blake, D.; Heikes, B.; Snow, J. *Nature* **2001**, *410*, 1078.
(3) Kley, D. *Science* **1997**, *276*, 1043.
(4) Finlayson-Pitts, B. J.; Pitts, J. N., Jr. *Science* **1997**, *276*, 1045.
(5) Wennberg, P. O.; Hanisco, T. F.; Jaegle, L.; Jacob, D. J.; Hintsa, E. J.; Lanzendorf, E. J.; Anderson, J. G.; Gao, R.-S.; Keim, E. R.; Donnelly, S. G.; DelNegro, L. A.; Fahey, D. W.; McKeen, S. A.; Salawitch, R. J.; Webster, C. R.; May, R. D.; Herman, R. L.; Proffitt, M. H.; Margitan, J. J.; Atlas, E. L.; Schauffler, S. M.; Flocke, F.; McElroy, C. T.; Bui, T. P. *Science* **1998**, *279*, 49.
(6) Barsanti, K. C.; Pankow, J. F. *Atmos. Environ.* **2004**, *38*, 4371.
(7) Khan, I.; Brimblecombe, P.; Clegg, S. L. *J. Atmos. Chem.* **1995**, *22*, 285.
(8) Lide, D.R., Ed. *CRC Handbook of Chemistry and Physics*, 85th ed.; CRC Press: Boca Raton, FL, 2004.
(9) Murphy, D. M.; Thomson, D. S.; Mahoney, M. J. *Science* **1998**, *282*, 1664.
(10) Murphy, D. M.; Thomson, D. S. *J. Geophys. Res.* **1997**, *102*, 6353.
(11) Lee, S.-H.; Murphy, D. M.; Thomson, D. S.; Middlebrook, A. M. *J. Geophys. Res.* **2002**, *107*, 1.
(12) Khare, P.; Kumar, N.; Kumari, K. M. *Rev. Geophys.* **1999**, *37*, 227.
(13) Chebbi, A.; Carlier, P. *Atmos. Environ.* **1996**, *30*, 4233.
(14) Nolte, C. G.; Solomon, P. A.; Fall, T.; Salmon, L. G.; Cass, G. R. *Environ. Sci. Technol.* **1997**, *31*, 2547.
(15) Tuazon, E. C.; Winer, A. M.; Pitts, J. N., Jr. *Environ. Sci. Technol.* **1981**, *15*, 1232.
(16) Talbot, R. W.; Sosher, B. W.; Heikes, B. G.; Jacob, D. J.; Munger, J. W.; Daube, B. C.; Keene, W. C.; Maben, J. R.; Artz, R. S. *J. Geophys. Res.* **1995**, *100*, 9335.
(17) Keene, W. C.; Galloway, J. N. *Atmos. Environ.* **1984**, *18*, 2491.
(18) Keene, W. C.; Galloway, J. N.; Holden, J. D., Jr. *J. Geophys. Res.* **1983**, *88*, 5122.
(19) Jacob, D. J. *J. Geophys. Res.* **1986**, *91*, 9807.
(20) Satsumabayashi, H.; Kurita, H.; Yokouchi, Y.; Ueda, H. *Tellus* **1989**, *41B*, 219.
(21) Neuman, J. A.; Nowak, J. B.; Brock, C. A.; Trainer, M.; Fehsenfeld, F. C.; Holloway, J. S.; Hübler, G.; Hudson, P. K.; Murphy, D. M.; Nicks, D. K., Jr.; Orsini, D.; Parrish, D. D.; Ryerson, T. B.; Sueper, D. T.; Sullivan, A.; Weber, R. *J. Geophys. Res.* **2003**, *108*, 4557.
(22) Sloane, C. S.; Watson, J.; Chow, J.; Pritchett, L.; Richards, L. W. *Atmos. Environ.* **1991**, *25A*, 1013.
(23) Gordon, R. J.; Bryan, R. J. *Environ. Sci. Technol.* **1973**, *7*, 645.
(24) Solomon, P. A.; Salmon, L. G.; Fall, T.; Cass, G. R. *Environ. Sci. Technol.* **1992**, *26*, 1594.
(25) Russell, A. G.; McRae, G. J.; Cass, G. R. *Atmos. Environ.* **1983**, *17*, 949.
(26) Chow, J. C.; Watson, J. G.; Fujita, E. M.; Lu, Z.; Lawson, D. R.; Ashbaugh, L. L. *Atmos. Environ.* **1994**, *28*, 2061.
(27) Watson, J. G.; Fujita, E. M.; Chow, J. C.; Zielinska, B.; Richards, L. W.; Neff, W.; Dietrich, D. *Northern Front Range Air Quality Study Final Report*; Desert Research Institute: Reno, NV, 1998.

(28) White, W. H.; Roberts, P. T. *Atmos. Environ.* **1977**, *11*, 803.
(29) Groblicki, P. J.; Wolff, G. T.; Countess, R. J. *Atmos. Environ.* **1981**, *15*, 2473.
(30) Prenni, A. J.; DeMott, P. J.; Kreidenweis, S. M.; Sherman, D. E.; Russell, L. M.; Ming, Y. *J. Phys. Chem. A* **2001**, *105*, 11240.
(31) Wise, M. E.; Surratt, J. D.; Curtis, D. B.; Shilling, J. E.; Tolbert, M. A. *J. Geophys. Res.* **2003**, *108*, article 4638.
(32) Kumar, P. P.; Broekhuizen, K.; Abbatt, J. P. D. *Atmos. Chem. Phys. Discuss.* **2003**, *3*, 949.
(33) Braban, C. F.; Abbatt, J. P. D. *Atmos. Chem. Phys.* **2004**, *4*, 1451.
(34) Cruz, C. N.; Pandis, S. N. *Environ. Sci. Technol.* **2000**, *24*, 4313.
(35) Shilling, J. E.; Tolbert, M. A. *J. Phys. Chem. A* **2004**, *108*, 11314.
(36) Xu, Q.; DeWitte, M.; Sloan, J. J. *Atmos. Environ.* **2003**, *37*, 911.
(37) Hudson, P. K.; Shilling, J. E.; Tolbert, M. A.; Toon, O. B. *J. Phys. Chem. A* **2002**, *106*, 9874.
(38) Koch, T. G.; Holmes, N. S.; Roddis, T. B.; Sodeau, J. R. *J. Chem. Soc Faraday Trans.* **1996**, *92*, 4787.
(39) Wexler, A. S.; Clegg, S. L. *J. Geophys. Res.* **2002**, *107*, 4207.
(40) Clegg, S. L.; Brimblecombe, P.; Wexler, A. S. *J. Phys. Chem. A* **1998**, *102*, 2137.
(41) Clegg, S. L.; Brimblecombe, P.; Wexler, A. S. *On-line Aerosol Inorganics Model. Model II: $H^+-NH_4^+$-$SO_4^{2-}-NO_3^--H_2O$ (180 to 330 K)*; Aerosol Inorganics Model Project/University of California: Davis, CA, 2005. Available at http://mae.ucdavis.edu/wexler/aim.
(42) Brooks, S. D.; Wise, M. E.; Cushing, M.; Tolbert, M. A. *Geophys. Res. Lett.* **2002**, *29*, 23.
(43) *TOXNET Toxicology Data Network*; NLM/NIH: Bethesda, MD, 2005. Available at http://toxnet.nlm.nih.gov, 2005 (accessed Aug 2005).
(44) Jayne, J. T.; Duan, S. X.; Davidovits, P.; Worsnop, D. R.; Zahniser, M. S.; Kolb, C. E. *J. Phys. Chem.* **1991**, *95*, 6329.
(45) Max, J.-J.; Chapados, C. *J. Phys. Chem. A* **2004**, *108*, 3324.
(46) Zondlo, M. A.; Barone, S. B.; Tolbert, M. A. *J. Phys. Chem. A* **1998**, *102*, 5735.
(47) Wexler, A. *J. Res. Natl. Bur. Stand.* **1976**, *73A*, 493.
(48) Lighstone, J. M.; Onasch, T. B.; Imre, D.; Oatis, S. *J. Phys. Chem. A* **2000**, *104*, 9337.
(49) Tabazadeh, A.; Toon, O. B. *Geophys. Res. Lett.* **1998**, *25*, 1379.
(50) Brandner, J. D.; Junk, N. M.; Lawrence, J. W.; Robins, J. *J. Chem. Eng. Data* **1962**, *7*, 227.
(51) Harned, H. S.; Ehlers, R. W. *J. Am. Chem. Soc.* **1933**, *55*, 652.
(52) Harned, H. S.; Ehlers, R. W. *J. Am. Chem. Soc.* **1933**, *55*, 2379.
(53) Harned, H. S.; Embree, N. D. *J. Am. Chem. Soc.* **1934**, *56*, 1042.
(54) Harned, H. S.; Sutherland, R. O. *J. Am. Chem. Soc.* **1934**, *56*, 2039.
(55) Beaucamp, S.; Bernand-Mantel, A.; Mathieu, D.; Agafonov, V. *Mol. Phys.* **2004**, *102*, 253.
(56) Christensen, J. C.; Hansen, L. D.; Izatt, R. M. *Handbook of Proton Ionization Heats and Related Thermodynamic Quantities*; John Wiley & Sons: New York, 1976.
(57) Romakkaniemi, S.; Hameri, K.; Vakeva, M.; Laaksonen, A. *J. Phys. Chem. A* **2001**, *105*, 8183.
(58) Weis, D. D.; Ewing, G. E. *J. Geophys Res.* **1999**, *104*, 21275.
(59) Foster, M. C.; Ewing, G. E. *J. Chem. Phys.* **2000**, *112*, 6817.
(60) Ewing, G. E. *J. Phys. Chem. B* **2004**, *108*, 15953.
(61) Tang, I. N.; Munkelwitz, H. R. *J. Geophys. Res.* **1994**, *99*, 18801.
(62) Saxena, P.; Hildemann, L. M. *J. Atmos. Chem.* **1996**, *24*, 57.
(63) Golden, D. M.; Iraci, L. T. Personal communication, 2005.
(64) Singleton, D. L.; Paraskevopoulos, G.; Irwin, R. S. *J. Am. Chem. Soc.* **1989**, *111*, 5249.
(65) Butkovskaya, N. I.; Kukui, A.; Pouvesle, N.; LeBras, G. *J. Phys. Chem. A* **2004**, *108*, 7021.